

Accepted: 11th May, 2025
Published: 29th May, 2025

Experimental and Surface Characterization of Quinazoline and its Derivatives as Corrosion Inhibitors for Mild Steel in 1 N HCl

**L. Hashim, I. Sani, A. Abubakar. Garba, A. Halilu Anka, and Z. M. Anka*

<https://doi.org/10.33003/frscs-2025-0402/03>

Abstract

Quinazoline (Qz), 2-Ethyl Quinazoline (2-E.Qz), and 2-Heptyl Quinazoline (2-H.Qz) were investigated as corrosion inhibitors for mild steel in 1 N HCl using gravimetric, electrochemical (potentiodynamic polarization, electrochemical impedance spectroscopy), and surface characterization by (SEM-EDX, contact angle) techniques. Inhibition efficiencies reached 79.31%, 88.50%, and 94.25% at 250 ppm for Qz, 2-E.Qz, and 2-H.Qz, respectively, with 2-H.Qz exhibiting superior performance due to enhanced physisorption via its heptyl substituent. Electrochemical analyses revealed mixed-type inhibition, with increased charge transfer resistance and reduced double-layer capacitance. SEM-EDX confirmed protective film formation, while contact angle measurements indicated a shift to hydrophobicity. Langmuir adsorption isotherms and negative Gibbs free energy values (-24.44 to -26.82 kJ/mol) supported physisorption. These findings highlight quinazoline derivatives as effective, eco-friendly inhibitors for mild steel protection in acidic environments, with potential applications in industrial corrosion mitigation.

Keywords: Quinazoline, Acidic Medium, Corrosion Inhibition, Mild Steel, EIS, SEM-EDX

Introduction

Mild steel is widely applied as a construction material in a larger number of industries due to its excellent mechanical properties and low cost. Although mild steel finds a wide range of technological applications, its poor corrosion resistance in acidic environments restrains its utility. Hydrochloric acid solutions are commonly used for pickling, industrial acid cleaning, acid de-scaling, and oil well acidifying processes. Because of the aggressiveness of acid solutions, mild steel corrodes severely during these processes, particularly with the use of hydrochloric acid, which results in a terrible waste of both resources and money. Therefore, a corrosion inhibitor is often added to the acid solutions to minimize the corrosion of mild steel in these processes. The selection of a good corrosion inhibitor is controlled by its economic availability, its efficiency to inhibit the substrate material, and its environmental side effects. The organic compounds containing nitrogen, Sulfur, and/or oxygen atoms have been reported as good inhibitors (Harsimran et al., 2021). For mild steel corrosion in an acidic environment. The inhibiting action of these compounds is due to the adsorption of these compounds to the metal/solution interface (Salazar-Jiménez et al., 2015).

1. Department of Chemistry, School of Science, Zamfara State College of Education, Maru PMB 1002, Nigeria

**Corresponding Author:*

L. Hashim
lawalhashim22@gmail.com

FRsCS Vol. 4 No. 2 (2025)
Official Journal of Dept. of Chemistry, Federal University of Dutsin-Ma, Katsina State.
<http://rscs.fudutsinma.edu.ng>

ISSN (Online): 2705-2362
ISSN (Print): 2705-2354

The adsorption process depends upon the nature and surface charge of the metal, the type of aggressive media, the structure of the inhibitor and the nature of its interaction with the metal surface (Jadhav et al., 2019). The quinazoline derivatives consist of 2-Ethyl quinazoline and 2-heptyl Quinazoline rings as well as a sufficient number of π -electrons, so it was expected that these compounds would be adsorbed on the metal surface and protect the metal from corrosion (Wasim et al., 2018). Therefore, in the present investigations, two quinazoline derivatives 2-Ethyl quinazoline and 2-heptyl quinazoline were synthesized and their corrosion inhibition performance was studied employing weight loss measurement, Potentiodynamic polarization, electrochemical impedance spectroscopy (EIS), and quantum chemical studies (Cai et al., 2018).

MATERIALS AND METHODS

Preparation Of The Mild Steel Specimens

To prepare the mild steel samples for weight loss analysis, they were polished using a polishing machine and emery sheets of 500, 600, and 800 grades. Mild steel size of 12.5 mm, 40 mm, and a thickness of 3 mm, after polishing, the specimens were washed with acetone and dried using a dryer. To prevent corrosion, the metal bars were stored in desiccators. These prepared samples were then used for a weight loss study.

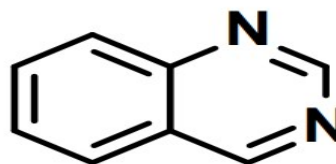
Preparation Of Stock Solutions

Conc. 1 N HCl Solution

Add 89 mL (milliliters) of hydrochloric acid (HCl) solution to a 1-liter standard measuring flask that previously contained a small quantity of distilled water. Shake the flask thoroughly to ensure even distribution

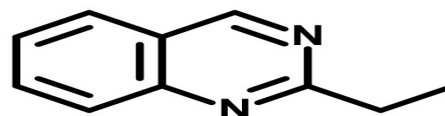
and homogeneity. Subsequently, top up the flask with additional distilled water until it reaches the marked level.

Quinazoline Inhibitor



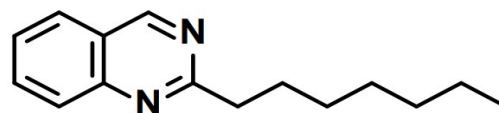
Place 1 g (gram) of quinazoline compound into a 100 ml (milliliter) standard measuring flask, and then add water until it reaches the indicated mark. Shake the flask thoroughly to ensure proper mixing.

2-Ethyl Quinazoline Inhibitor



Take 1 g(gram) of ethyl quinazoline compound into a 100 ml (milliliter) standard measuring flask, then add water until it reaches the indicated mark. Shake the flask thoroughly to ensure proper mixing (Mohammed et al., 2023).

2-Heptyl Quinazoline Inhibitor.



Place 1 g (gram) of ethyl quinazoline compound into a 100 ml (milliliter) standard measuring flask, and then add water until it reaches the indicated mark. Shake the flask thoroughly to ensure proper mixing (Ferigita et al., 2022).

Metal Composition

Table 1: Metal Composition

S. No.	COMPOUND	PERCENTAGE
1	Carbon	0.116
2	Manganese	0.85
3	Sulphur	0.007
4	Phosphorous	0.0024

Weight Loss Method

Weighing Specimens Before And After Corrosion

The weight of the metal samples before and after being submerged is determined using a weighing machine.

Determination Of Corrosion Rate

Gravimetric Experiments were conducted according to established protocols. This method is commonly employed and offers a dependable approach for evaluating the corrosion rate of a given sample. The samples underwent analysis in a solution of 1 N HCl both with and without varying concentrations of inhibitors (50, 100, 150, 200, and 250 ppm) at room temperature (30°C) for one hour. Mild steel specimens were immersed for the designated duration, then extracted, and their surfaces thoroughly rinsed with distilled water, dried with cool air, and subsequently weighed on a precision balance. Usman, A. D., at., el. 2015). The corrosion rate (CR) and inhibition efficiency (IE %) were determined by assessing the weight variances obtained through a specified method. The corrosion rate is computed using the formula: CORROSION RATE (mm/y) = $87.6 * W \text{ (mg)} / ADT \text{ (H)}$, where W represents the weight loss in milligrams (mg), D is the metal density in

g/cm³, A denotes the sample area in cm², and T signifies the exposure time of the metal sample in hours (1h). (Kadhim et al., 2021).

$$CR \text{ (mm/y)} = \frac{W \times K}{D \times A \times T}$$

(1)

$$I.E \text{ (%) } = \frac{W_0 - W_1}{W_0} \times 100$$

(2)

Electrochemical Studies

The Electrochemical Tests (PDP and EIS)

were conducted using a ~~Bio-Logic SP 300~~ and a three-electrode cell setup. This setup included mild steel coupons as the working electrode, a saturated calomel electrode (SCE) as the reference electrode, and platinum as the counter electrode. The experiments took place in a 1 N hydrochloric acid solution with varying concentrations of Qz, 2-E.Qz and 2-H.Qz at 30°C. Scully et al., 2022) Before testing, the three-electrode system was immersed in the corrosive solution for 5 minutes to stabilize the open-circuit potential (Eocp). PDP assessments were performed within a potential range of ±250 mV around the corrosion potential equilibrium, using a scan rate of 1 mV/s. EIS analyses covered frequencies from 100 kHz to 0.01 Hz with 10 mV AC signals. The effectiveness of corrosion inhibition, as determined from the PDP and EIS data, is assessed using specific equations. (Shreir, L. L. at., el. 2013).

$$IE_{PDP} \% = \frac{I_{corr} - I_{corr}^0}{I_{corr}} \times 100\%$$

(3)

Where:

I_{corr}^* = current density with inhibitor

I_{corr} = current density without inhibitor

$$IE_{EIS}\% = \frac{R_{ct} - R_{ct}^0}{R_{ct}} \times 100\% \quad (4)$$

R_{ct}^0 = the charge – transfer resistance without inhibitor

R_{ct} = the charge – transfer resistance with the inhibitor

Surface Characterisation Studies

SEM

Surface analysis was conducted using a Scanning Electron Microscope (SEM) SNE-3200 M from “SEC Global PVT Ltd”, equipped which has an in-built energy dispersive X-ray Analyzer. Metal samples were immersed in 1 N HCl for one hour at room temperature, first in a non-inhibited solution and secondly in inhibited solutions containing a 250 parts per million concentration. Rephrased: The chemical composition of the test samples was analysed utilizing an Energy-dispersive X-ray analyser (EDAX). (Ma et al., 2022).

Contact Angle Measurements

Contact angle assessments were conducted on mild steel samples prepared in a manner consistent with those utilized in the polarization test. The water contact angle (WCA) was determined on mild steel surfaces using a KYOWA DMs-40 contact angle meter, employing the half-angle technique fitting and FAMAS software for interface measurement and analysis. Mild steel vouchers were submerged in the test solution for 1 hour at 30°C with an optimized inhibitor concentration. (Betti, N., et al., 2021).

RESULTS AND DISCUSSION

Quinazoline And Its Derivatives' Inhibition Of Corrosion On Mild Steel In An Acidic Environment:

An Experiment Using the Gravimetric Method.

During a gravimetric experiment, mild steel samples were submerged in 1 N HCl solutions containing different concentrations of Quinazoline and its derivatives for 1 hour at a temperature of 30°C. The corrosion rate (CR), inhibitory efficiency (IE), and weight loss were measured and displayed in Table 2. (Subasree, N., et al., 2020). Figure 1 demonstrates the influence of Quinazoline and its variants on CR and IE. The inhibitory effectiveness was shown to be positively correlated with higher concentrations of the inhibitor, suggesting that there was a sufficient amount of inhibitor present to provide efficient coverage on the surface of the mild steel. Qz, 2-E.Qz, and 2-H.Qz exhibited inhibitory efficiency that varied with the concentration. The highest levels of inhibitory effectiveness were observed at concentrations of 250 ppm for Qz, 2-E.Qz, and 2-H.Qz, with inhibitory efficiencies of 79.31%, 88.50%, and 94.25% correspondingly (Errahmany et al., 2020). The different levels of corrosion inhibition efficiency exhibited by Qz, 2-E.Qz, and 2-H.Qz can be due to the distinct substituent groups present on the benzene ring, as visible in the chemical structure of these inhibitors. These substituents impart the benzene ring with an electrophilic heteroatom (either oxygen or nitrogen) that possesses an additional pair of electrons (Laabaissi et al., 2020). This increases the electron density and strengthens the inhibitory effect of the inhibitor molecules. (Sayyid et al., 2022). As the concentration of inhibition increases, there is a corresponding decrease in weight loss and

an enhancement in inhibition efficiency. The observed surface coverage is attributed to the interaction between metal ions and the

corrosion inhibitor molecule (Ravi et al., 2023).

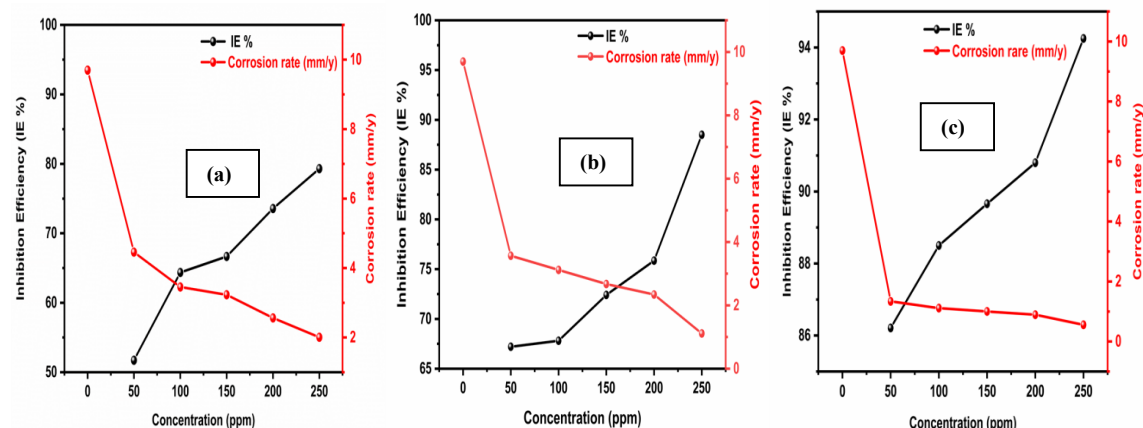


Figure 5.1 displays the correlation between corrosion rates and inhibition efficiency at different concentrations of Qz, 2-E.Qz, and 2-H.Qz inhibitors, as determined using the weight loss method at 30°C in 1 N HCl medium

Temperature's Impact

A series of gravimetric studies was conducted to investigate the influence of temperature on corrosion and inhibition efficiency. (Chen et al., 2021) The experiments were carried out within a temperature range of 40 to 60°C. The findings, outlined in Table 1, demonstrate that the corrosion rate (CR) of mild steel in acidic solutions decreases as the concentrations of Qz, 2-E.Qz, and 2-H.Qz increase. (Kumar et al., 2020). This indicates that the inhibitors, specifically Quinazoline and its derivatives, successfully reduced the rate of deterioration of mild steel in an acidic solution in a manner that depended on the concentration. (Lgaz et al., 2017) The inhibition of this process is caused by the adsorption of inhibitor molecules onto the surface of the mild steel. This adsorption creates a protective layer that covers the reactive sites of the exposed

specimen in a hydrochloric acid solution with a concentration of 1 N. The shielding effect results in a reduction in the rate of corrosion and an improvement in the effectiveness of protection as the concentration of the inhibitor increases. Remarkably, the study found that rising temperatures resulted in elevated corrosion rates in both uncontrolled and inhibited solutions. This suggests that when the temperature and agitation of the corrosive fluid increase, the steel becomes more vulnerable to deterioration. Furthermore, it was observed that the inhibitory efficacy decreases as the temperature increases, which is a typical feature related to the adsorption of molecules by weak physical forces. (Xu et al., 2023). To summarize, the research emphasizes the significance of taking temperature effects into account when evaluating corrosion inhibition tactics.

Table 1: Temperature Effects

Temperature (°C)	Corrosion rate (mm/y)						Inhibition Efficiency (IE %)		
	Blank			250 ppm					
	Q	2-EQ	2-HQ	Q	2-EQ	2-HQ	Q	2-EQ	2-HQ
30	9.6962	9.6962	9.6962	2.0061	1.1145	0.5573	79.31	88.50	94.25
40	10.8106	10.8106	10.8106	4.7923	4.1236	3.0091	55.67	61.85	73.19
50	13.3740	13.3740	13.3740	8.4702	6.4641	5.4610	36.66	51.66	59.166
60	16.3832	16.3832	16.3832	11.8137	9.4732	7.5786	27.89	42.17	53.74

It highlights the intricate relationship between temperature, inhibitor concentration, and corrosion rates in protecting metals. (Aslam et al., 2020).

Analysis Of Electrochemical Phenomena An Investigation Using Potentiodynamic Polarization

To study the behaviour of mild steel in hydrochloric acid solutions containing quinazoline and its derivatives. The study performed Potentiodynamic polarization analysis on mild steel submerged in hydrochloric acid solutions with different concentrations of Qz, 2-E.Qz, and 2-H.Qz at a temperature of 30°C. The current-potential curves acquired provided insight into the electrochemical characteristics of the system. The corrosion potential (E_{corr}), anodic and cathodic Tafel slopes (β_a and β_c), corrosion current density (I_{corr}), and inhibition efficiency (I. E %) were measured and presented in Table 2. Understanding the Mechanism and Efficiency of Inhibition. The process of inhibition had a direct relationship with concentration, where higher concentrations of inhibitors resulted

in greater efficiency of inhibition. At first, the inhibitors attached to the surface of the mild steel, blocking the active sites that cause corrosion. This action led to a significant reduction in both the current densities of the anodic and cathodic reactions, suggesting the inhibition of the dissolution of mild steel and the reduction of hydrogen ions, respectively. The inhibitors acted as mixed-type inhibitors, as demonstrated by their influence on the electrochemical processes. Categorization of Inhibitors The change in (E_{corr}) values was essential in classifying the inhibitors as anodic, cathodic, or mixed type. A E_{corr} A difference greater than 85 mV between inhibited and unfettered systems indicates either anodic or cathodic behavior, whereas shifts below 85 mV classify the inhibitors as mixed type. The Quinazoline compounds that were studied were shown to be mixed-type inhibitors, with a predominant tendency to exhibit anodic properties. Formation of a protective barrier. The inhibitors effectively decreased the corrosion current density values, with 2-H. Qz exhibiting the lowest

(I_{corr}), indicating a significant deceleration in the electrochemical process. The decrease in the rate of corrosion was ascribed to the development of a defensive inhibitor layer on the surface of the metal, which functions as a barrier against the destructive

surroundings. In summary, the study demonstrated that Qz, 2-E.Qz, and 2-H.Qz are effective inhibitors with mixed-type properties. These inhibitors have the potential to reduce corrosion in harsh acid solutions (Mashuga et al., 2015).

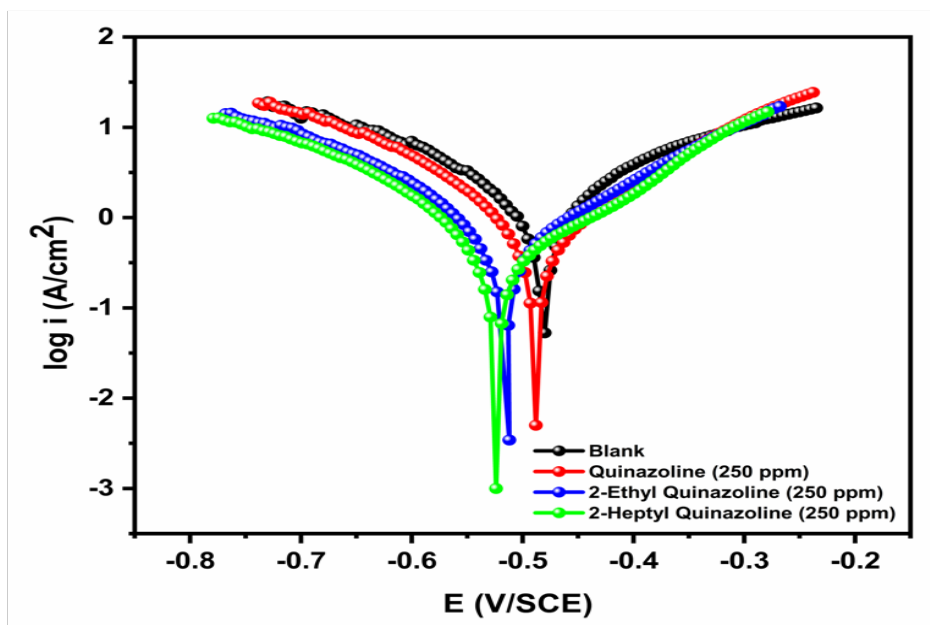


Fig 2 for blank, Qz (250ppm), 2-E. Qz(250ppm), and 2-H.Qz (250ppm)

Table 2: Potentiodynamic Polarization

Inhibitor	$-E_{corr}$ (mV vs SCE)	I_{corr} ($\mu\text{A}/\text{cm}^2$)	R_p (Ω / cm^2)	β_a (mV dec^{-1})	$-\beta_c$ (mV dec^{-1})	CR (mm/y)	IE (%)
Blank	481	135.41	10.17	296	279	13.53	-
Qz (250 ppm)	487	32.5	67.86	226	238	4.26	75.99
2-E.Qz (250ppm)	513	18.22	115.5	236	227	2.06	86.54
2-H. Qz (250ppm)	523	6.99	318.6	258	249	3.95	94.83

Electrochemical Impedance Spectroscopy (Eis)

Electrochemical Impedance Spectroscopy (EIS) is a highly effective method employed for investigating the electrochemical characteristics of materials in different surroundings. The corrosion inhibition process of mild steel samples submerged in 1 N HCl solutions with and without inhibitors, such as Qz, 2-E.Qz, and 2-H.Qz, at a temperature of 30 °C can be better understood by the analysis of Nyquist and Bode plots. Figure 3 shows the Nyquist plots. Both the unconstrained and inhibited solutions display a semicircular capacitive loop in the Nyquist plots across the entire frequency range under study (Saha et al., 2018). The inclusion of inhibitors, specifically Qz, 2-E.Qz, and 2-H.Qz, leads to the formation of bigger semicircles in comparison to the system without inhibitors. As the concentrations of the corrosion inhibitors increase, the size of the semicircle also increases, which suggests improved corrosion protection. The Nyquist graphs indicate the presence of one-time constant phase elements in both the blank and inhibited systems. The equivalent circuit shown in Figure 5 consists of three components: solution resistance (R_{ct}), double-layer capacitance (C_{dl}), and charge transfer resistance (R_{ct}). The experimental data strongly correlate with this circuit model, validating its relevance to the observed electrochemical activity. The existence of inhibitors results in an elevated charge transfer resistance (R_{ct}), which signifies enhanced corrosion protection for the mild steel samples. Bode phase plots: The Bode phase plots depicted in Figure 4

exhibit a singular time- constant behaviour when inhibitors are present. As the concentration of inhibitors rises, the phase angle peak shifts towards a more negative direction, indicating improved inhibition efficiency. In summary, the results demonstrate that Qz, 2-E.Qz, and 2-H.Qz is effective in preventing corrosion of mild steel in acidic conditions, as indicated by the observed alterations in the electrochemical impedance spectroscopy (EIS) measurements. A higher concentration of inhibitors can result in a more potent inhibitory effect, as seen by a larger negative phase angle value. In the field of corrosion studies, the values of charge transfer resistance (R_{ct}) play a vital role in determining the effectiveness of inhibitors. When inhibitors such as Qz, 2-E.Qz, and 2-H.Qz are added to a solution, the R_{ct} value experience a large rise in comparison to systems without inhibitors. This indicates the development of protective layers on the surface of the metal. The rise in R_{ct} Values are linked to a decline in the double-layer capacitance (C_{dl}), potentially caused by alterations in the local dielectric constant or the thickness of the electric double layer. These inhibitors work by adhering to the interface of the metal surface, resulting in enhanced efficiency in preventing corrosion as the concentrations increase. The highest levels of inhibition were found in Table 3, with Qz and 2-E.Qz in shows a maximum efficiency of 74.03%, and 2-H.Qz shows an efficiency of 85.43% and 92.47% respectively. These best results were achieved at a concentration of 250 ppm. Impedance spectroscopy investigations corroborate the findings of polarization and

weight loss trials, providing more evidence of the inhibitory properties of these substances. Nevertheless, the presence of constraints in the binding of inhibitors to

metal surfaces can impede the attainment of optimal inhibition efficiency, even in the presence of inhibitors with advantageous characteristics (Subasree et al., 2023).

Table 3: Parameters for Electrochemical Impedance Spectroscopy

Inhibitors	$R_{ct} (\Omega \text{ cm}^2)$	$C_{dl} (\text{F cm}^{-2})$	IE (%)
Blank	51.93	3.809×10^{-4}	-
Qz (250 ppm)	199.98	3.005×10^{-4}	74.03
2-E.Qz (250 ppm)	356.44	2.749×10^{-4}	85.43
2-H.Qz (250 ppm)	689.85	2.545×10^{-4}	92.47

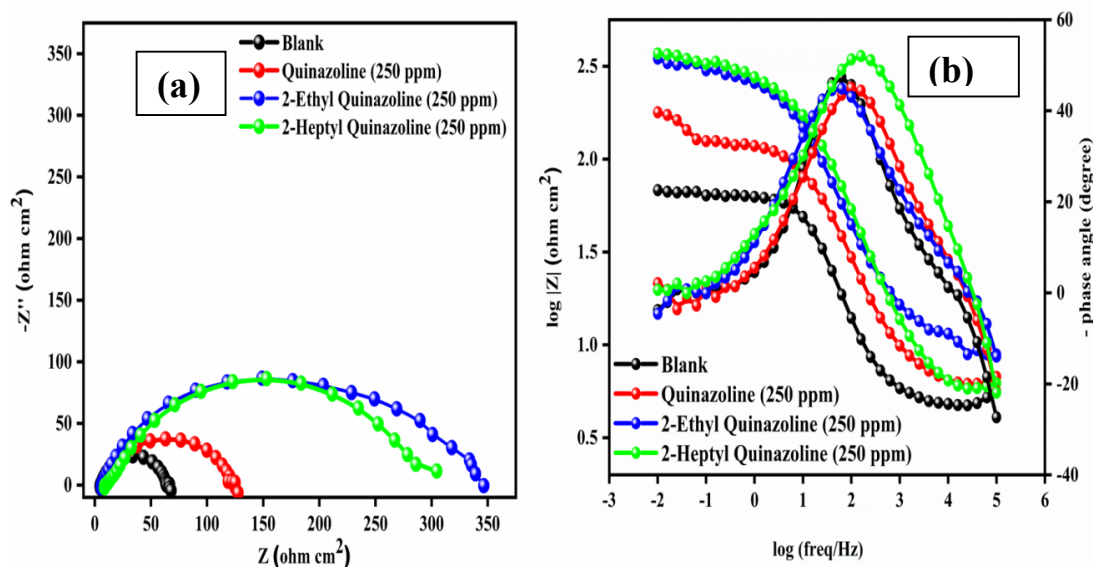


Fig.3 (a). Nyquist plots for MS with and without Qz, 2-E.Qz and 2-H.Qz in 1 N HCl medium for the concentrations of (250 ppm) at 30 °C. Fig. 3(b). Bode plots for MS with and without Qz, 2-E.Qz and 2-H.Qz in 1 N HCl electrolyte for concentrations OF 250 ppm) at 30 °C.

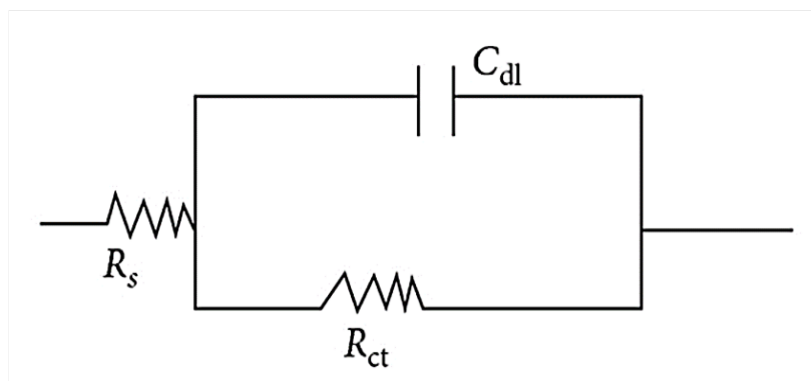


Figure 5: Equivalent Circuit

The Adsorption Isotherm

The ability of organic molecules to prevent corrosion is determined by their adsorption capability on metal surfaces. Adsorption isotherms can yield significant and valuable information. The adsorption isotherms, namely Langmuir, Freundlich, and Temkin, were examined by utilizing surface coverage values (θ) obtained from weight loss experiments. It was determined that the Langmuir adsorption isotherm was followed (Bashir et al., 2021). The Langmuir adsorption isotherm is a linear graph that shows the relationship between the concentration of the corrosion inhibitor (C) and the surface coverage (θ), as depicted in Figure 6. The adsorption constant (k_{ads}) of the inhibitor was determined using the equation: $k_{ads} = \frac{C}{\theta}$, where θ represents the degree of surface coverage, C is the concentration of the inhibitor, and k_{ads} it is the equilibrium constant of the adsorption/desorption process. K_{ads} is calculated based on the intercept obtained from Figure 6. The correlation coefficient (R^2) values of 0.9885, 0.9918, and 0.9998 for Qz, 2-E.Qz, and 2-H.Qz at 30°C demonstrates a strong agreement with the

Langmuir adsorption isotherm. This suggests that the adsorption capacity of Qz, 2-E.Qz, and 2-H.Qz on the surface of mild steel is high. Table 4 unambiguously demonstrates a negative correlation between temperature and k_{ads} , suggesting that the molecules of inhibitors that adhere to the steel surface become detached as the temperature increases. The k_{ads} can be associated with the variation in Gibbs' adsorption free energy (ΔG_{ads}°) and is determined using the following equation: R represents the universal gas constant, T represents the absolute temperature, and ΔG_{ads}° represents the free energy of adsorption. The value 1000 represents the molar concentration of water in bulk solution, measured in grams per liter (or milliliters per liter). If the values of ΔG_{ads}° are -24 kJ/mol and -25 kJmol^{-1} , or less negative, it indicates physisorption resulting from the electrostatic contact between the inhibitor and the charged surface of mild steel. Conversely, a value of ΔG_{ads}° equal to or less than -40 kJmol^{-1} indicates chemisorption, where there is electron sharing or charge transfer from the organic

compound to the metal surface. In this study, the value of ΔG_{ads}° is below -20 kJ mol^{-1} , suggesting that the adsorption is of a physical nature. Consequently, the inhibitors that were studied were shown to be physically adsorbed onto the surface of the metal. The occurrence of the adsorption process on the mild steel surface is demonstrated by the presence of negative values of free energy adsorption (ΔG_{ads}°). As the temperature increases, the effectiveness of inhibition will diminish. The physisorption of inhibitor compounds is

primarily influenced by the molecule's structure and the electron density of the donor atom. Interestingly, the standard Gibbs free energy change (ΔG_{ads}°) value for 2-H.Qz is approximately $-26.82 \text{ kJ mol}^{-1}$ higher than that of Qz and 2-E.Qz. The higher adsorption value indicates the presence of the amino group in 2-H.Qz has enhanced the capacity for physisorption. This phenomenon occurs when the N atom of the heteroatom travels towards the metal surface during adsorption. When comparing Qz with 2-E.Qz. (Hrimla et al., 2020).

Table 4: The Adsorption Isotherm Value

Inhibitor	T (°C)	R ²	K _{ads} (Lg ⁻¹)	ΔG_{ads}° (kJ mol ⁻¹)
Quinazoline	30	0.9885	42.15	-24.44
2-Ethyl quinazoline	30	0.9918	21.42	-25.12
2-Heptyl quinazoline	30	0.9995	16.35	-26.82

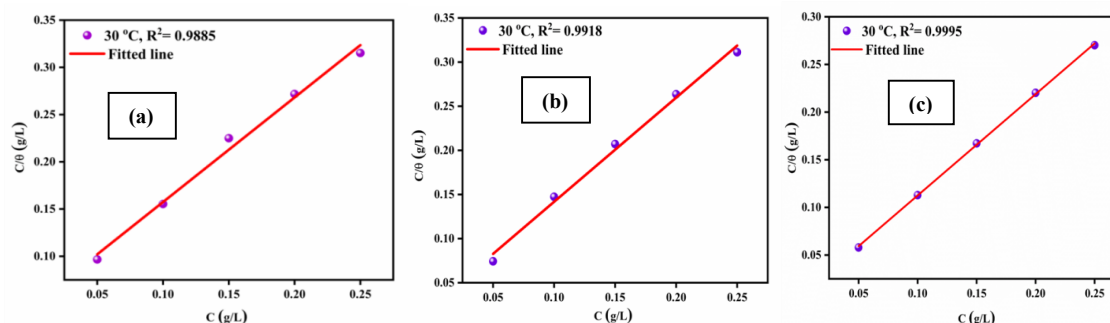


Figure 6 displays the Langmuir adsorption isotherm of mild steel in a 1 N HCl solution. The graph shows three different inhibitors: Qz, 2-E.Qz, and 2-H.Qz, all tested at a temperature of 30°C.

Measurement Of Contact Angle

Contact angle (CA) measurements offer additional understanding of material surface phenomena, including adsorption, wetting,

and adhesion. The contact angle was measured to examine the influence of the adsorption layer on the degree of hydrophobicity or hydrophilicity of the mild

steel samples (Ravi et al., 2023). Figure 8 displays the contact angle measurement of the mild steel surface when it is submerged in a 1 N HCl solution, both with and without the presence of an inhibitor. The recently polished mild steel surface exhibits hydrophobic qualities, with a contact angle value of 107.8° , as depicted in Figure 8a. After immersing a mild steel surface in a 1 N hydrochloric acid solution for 1 hour, the contact angle decreased to 72.9° , which is similar to the hydrophilic nature of the corrosion products on the metal surface (Fig. 8b). The corrosion products created mostly consist of polar substances, which in turn cause changes to the composition and

features of the surface. Consequently, water droplets on the surface are easily deformed. Nevertheless, the aggressive solution was supplemented with 250 ppm of Qz, 2-E.Qz, and 2-H.Qz, resulting in an increase in the contact angle value by 92.7° , 101.8° , and 102.9° correspondingly, as depicted in Figure 8c, d, and e. The wettability of the metal was reduced by forming a layer of inhibitors on the surface of the mild steel, resulting in its conversion to a hydrophobic state. This study examines how the presence of corrosion inhibitor molecules in an acidic environment transforms a hydrophilic surface into a hydrophobic one (Zhao, T., 2018).

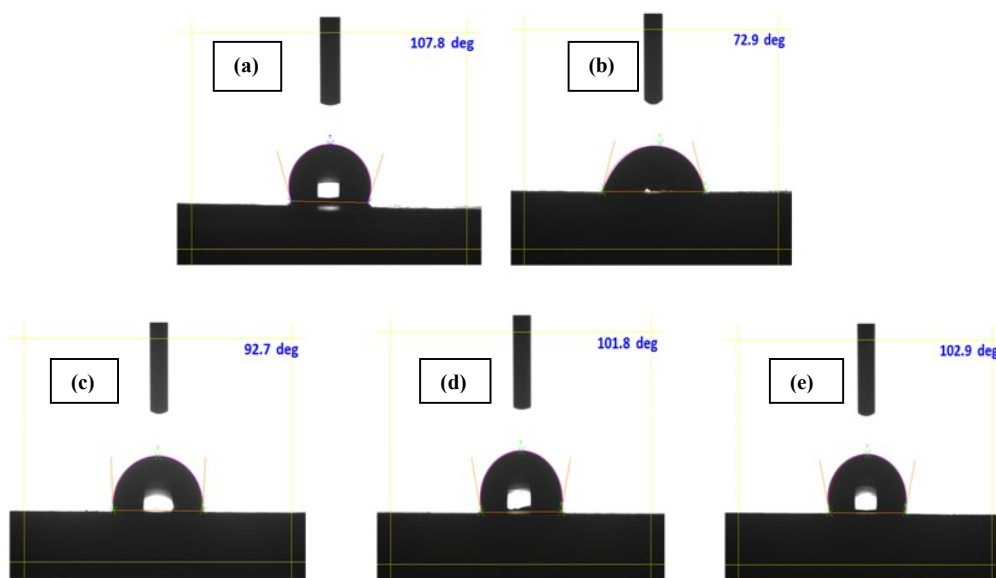


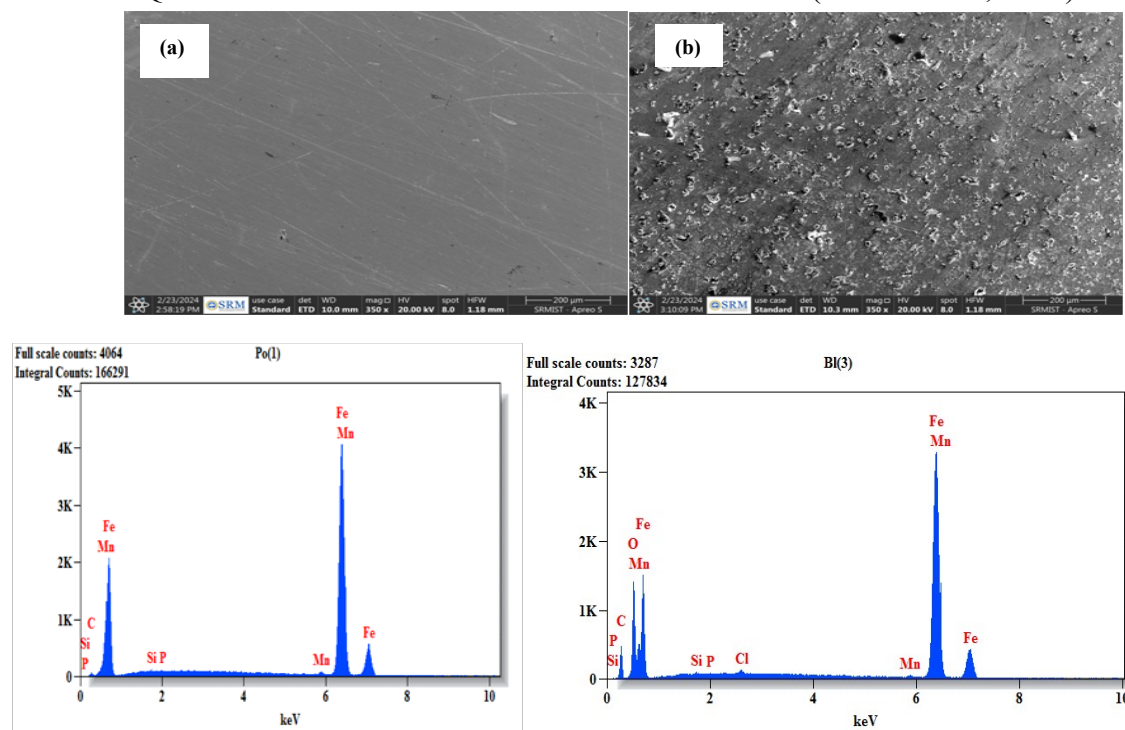
Figure 7 shows the contact angle measurement of mild steel at a temperature of 30°C . The measurements include: (a) polished mild steel, (b) mild steel immersed in 1 N HCl, (c) mild steel submerged in 250 ppm of Qz, (d) mild steel immersed in 250 ppm of 2-E.Qz, and (e) mild steel immersed in 250 ppm of 2-H.Qz.

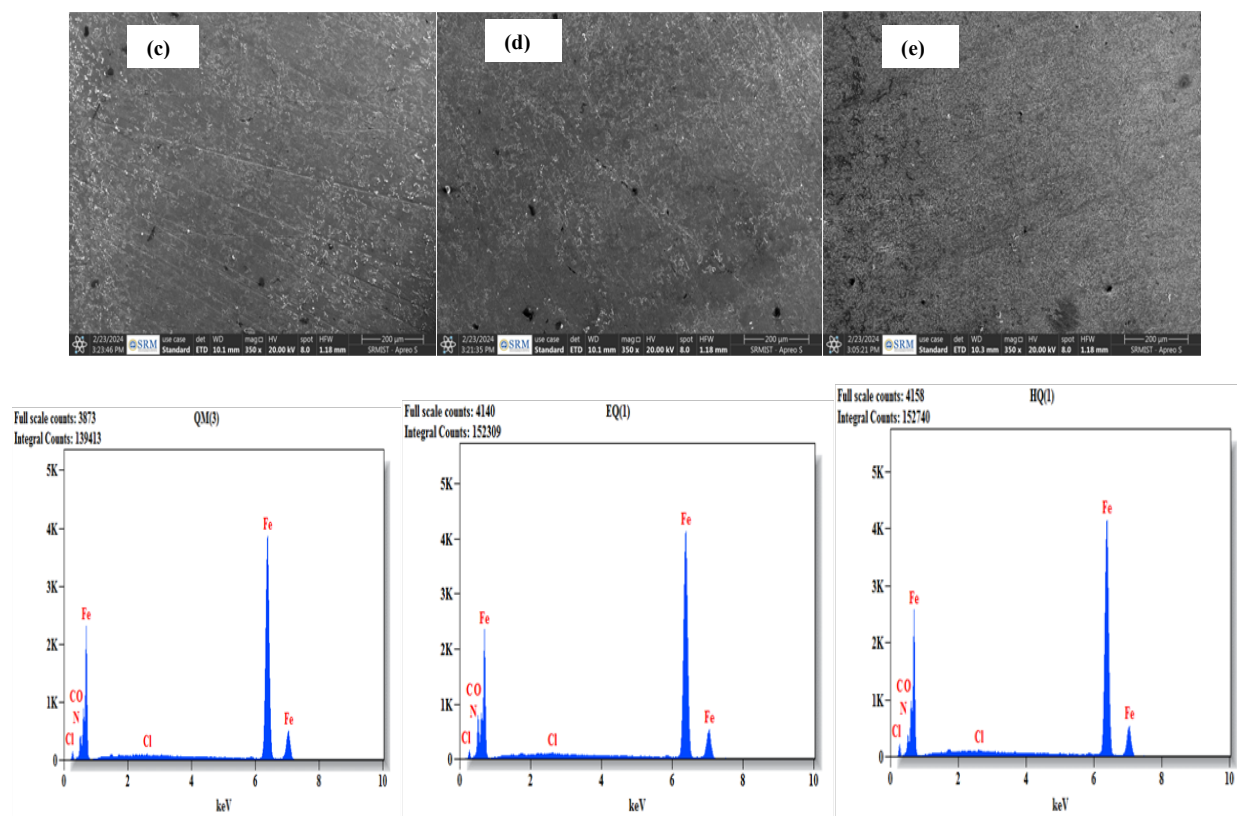
Analysis Of The Surface Using Scanning Electron Microscopy With Energy-Dispersive X-Ray Spectroscopy (SEM-EdAX).

The outer surface morphology of mild steel specimens immersed in a 1 N HCl solution was analyzed using Scanning Electron Microscopy (SEM). (Wang, Y., et al., 2018).

2023). The specimens were tested in both uninhibited and inhibited solutions containing 250 ppm of Qz, 2-E.Qz, and 2-H.Qz for 1 hour at a temperature of 30°C. The results of this analysis may be seen in Figures 9 and 10. Without an inhibitor, the surfaces of the mild steel experienced significant damage and extensive corrosion as a result of the quick dissolution of iron in a corrosive environment. However, when comparing it to the blank solution (Fig. 9), the inclusion of 250 ppm of Qz, 2-E.Qz, and 2-H.Qz inhibits the corrosion rate and greatly diminishes surface damage (Figs. 9 and 10). The production of a protective inhibitor coating on the surface of mild steel is related to the adsorption of Qz, 2-E.Qz, and 2-H.Qz. The EDAX table 5 data

provides information on the elemental makeup of carbon, oxygen, nitrogen, and iron atoms obtained from both the inhibited and uninhibited metal surfaces. Without inhibitors, the elemental composition and spectra suggest a significant proportion of iron (Fe) and minimal amounts of carbon (C), oxygen (O), and nitrogen (N). This could be attributed to the generation of oxides, specific mild steel composites, or the electrolyte (Alrefae et al., 2020). When an inhibitor is present, the adsorbed Qz, 2-E.Qz, and 2-H.Qz on the mild steel surfaces changes the elemental composition of Fe and increases the presence of C, N, and O atoms. This change in composition enhances the mild steel's ability to protect against corrosion (Ouakki et al., 2021).





Figures 8 and 9 show scanning electron microscopy-energy dispersive X-ray spectroscopy (SEM-EDX) pictures of mild steel at a temperature of 30°C. Image (a) displays polished mild steel, image (b) shows mild steel immersed in 1 N hydrochloric acid (HCl), image (c) depicts mild steel submerged in 250 parts per million (ppm) of Qz, and image (d) illustrates mild steel immersed in 250 ppm of 2-E. Qz, and image (e) exhibit mild steel immersed in 250 ppm of 2-H. Qz.

Table 5 displays the EDAX values.

Weight (%)	Polished metal	Blank (0 ppm)	Quinazoline	2-Ethyl quinazoline	2-Heptyl quinazoline
C	1.12	6.15	2.31	2.21	3.22
N	—	—	0.35	0.40	0.41
O	—	12.25	5.38	2.78	2.27
Fe	97.86	80.49	94.52	91.92	93.98

CONCLUSION

The corrosion inhibitory properties of quinazoline and its derivatives, including Qz, 2-E.Qz, and 2-H.Qz, has been examined in a 1 N HCl solution using weight loss, electrochemical, and surface analysis techniques, where 2-H.Qz exhibits a maximum inhibitory efficiency of 94.25% at a concentration of 250ppm in a 1 N HCl solution at normal room temperature on a mild steel surface, Hence an electrochemical polarization analysis indicates that the inhibitors used exhibit mixed-type behaviour, Electrochemical impedance analysis demonstrates that the utilization of inhibitors leads to a considerable rise in charge transfer values and a decrease in double layer capacitance values in a 1N HCl solution. This indicates that the corrosion inhibitors are adsorbed onto the surface of the metal. SEM-EDX analyses were conducted to verify the adsorption and protection efficacy of quinazoline and its derivatives on mild steel in a 1 N HCl solution and Formation of a protective layer on mild steel was characterized by Contact Angle measurement. Hence, this research confirms that 2-H.Qz is the best inhibitor and further research can be carried out to ascertain its full potential.

Reference:

- Abdolkarimi-Mahabadi, M., Bayat, A., & Mohammadi, A. (2021). Use of UV-Vis spectrophotometry for characterization of carbon nanostructures: a review. *Theoretical and Experimental Chemistry*, 57, 191-198
- Aslam, J., Aslam, R., Alrefaee, S. H., Mobin, M., Aslam, A., Parveen, M., & Hussain, C. M. (2020). Gravimetric, electrochemical, and morphological studies of an isoxazole derivative as corrosion inhibitor for mild steel in 1M HCl. *Arabian Journal of Chemistry*, 13(11), 7744-7758.
- Bashir, S., Lgaz, H., Chung, I. M., & Kumar, A. (2021). Effective green corrosion inhibition of aluminium using analgin in acidic medium: an experimental and theoretical study. *Chemical Engineering Communications*, 208(8), 1121-1130.
- Cai, Y., Zhao, Y., Ma, X., Zhou, K., & Chen, Y. (2018). Influence of environmental factors on atmospheric corrosion in dynamic environment. *Corrosion Science*, 137, 163-175
- Chen, W., Nie, B., Liu, M., Li, H. J., Wang, D. Y., Zhang, W., & Wu, Y. C. (2021). Mitigation effect of quinazolin-4 (3H)-one derivatives on the corrosion behavior of mild steel in HCl. *Colloids and Surfaces A: Physicochemical and Engineering Aspects*, 627, 127188
- Errahmany, N., Rbaa, M., Abousalem, A. S., Tazouti, A., Galai, M., Touhami, M. E., & Tour, R. (2020). Experimental, DFT calculations and MC simulations concept of novel quinazolinone derivatives as corrosion inhibitor for mild steel in 1.0 M HCl medium. *Journal of Molecular Liquids*, 312, 113413.
- Feng, L., Zhang, S., Qiang, Y., Xu, S., Tan, B., & Chen, S. (2018). The synergistic corrosion inhibition study of different

- chain lengths ionic liquids as green inhibitors for X70 steel in acidic medium. *Materials Chemistry and Physics*, 215, 229-241.
- Ferigita, K. S. M., AlFalah, M. G. K., Saracoglu, M., Kokbudak, Z., Kaya, S., Alaghani, M. O. A., & Kandemirli, F. (2022). Corrosion behaviour of new oxo-pyrimidine derivatives on mild steel in acidic media: Experimental, surface characterization, theoretical, and Monte Carlo studies. *Applied Surface Science Advances*, 7, 100200.
- Fouda, A. S., El-Desoky, A. M., & Hassan, H. M. (2013). Quinazoline derivatives as green corrosion inhibitors for carbon steel in hydrochloric acid solutions. *International Journal of Electrochemical Science*, 8(4), 5866-5885.
- Groysman, A., & Groysman, A. (2010). Corrosion mechanism and corrosion factors. *corrosion for everybody*, 1-51.
- Harsimran, S., Santosh, K., & Rakesh, K. (2021). Overview of corrosion and its control: A critical review. *Proc. Eng. Sci*, 3(1), 13-24.
- Hrimla, M., Bahsis, L., Boutouil, A., Laamari, M. R., Julve, M., & Stiriba, S. E. (2020). A combined computational and experimental study on the mild steel corrosion inhibition in hydrochloric acid by new multifunctional phosphonic acid containing 1, 2, 3-triazoles. *Journal of Adhesion Science and Technology*, 34(16), 1741-1773.
- Jadhav, N., & Gelling, V. J. (2019). The use of localized electrochemical techniques for corrosion studies. *Journal of the Electrochemical Society*, 166(11), C3461.
- Kadhim, A., Betti, N., Al-Bahrani, H. A., Al-Ghezi, M. K. S., Gaaz, T., Kadhum, A. H., & Alamiery, A. (2021). A mini review on corrosion, inhibitors and mechanism types of mild steel inhibition in an acidic environment. *International Journal of Corrosion and Scale Inhibition*, 10(3), 861-884.
- Kumar, C. P., Prashanth, M. K., Mohana, K. N., Jagadeesha, M. B., Raghu, M. S., Lokanath, N. K., & Kumar, K. Y. (2020). Protection of mild steel corrosion by three new quinazoline derivatives: experimental and DFT studies. *Surfaces and Interfaces*, 18, 100446.
- Laabaissi, T., Benhiba, F., Missioui, M., Rouifi, Z., Rbaa, M., Oudda, H., & Zarrouk, A. (2020). Coupling of chemical, electrochemical and theoretical approach to study the corrosion inhibition of mild steel by new quinoxaline compounds in 1 M HCl. *Heliyon*, 6(5).
- Lgaz, H., Salghi, R., Bhat, K. S., Chaouiki, A., & Jodeh, S. (2017). Correlated experimental and theoretical study on inhibition behavior of novel quinoline derivatives for the corrosion of mild steel in hydrochloric acid solution. *Journal of Molecular Liquids*, 244, 154-168.
- Ma, I. W., Ammar, S., Kumar, S. S., Ramesh, K., & Ramesh, S. (2022). A concise review on corrosion inhibitors: types, mechanisms and electrochemical evaluation studies.

- Journal of Coatings Technology and Research, 1-28.
- Mashuga, M. E., Olasunkanmi, L. O., Adekunle, A. S., Yesudass, S., Kabanda, M. M., & Ebenso, E. E. (2015). Adsorption, thermodynamic and quantum chemical studies of 1-hexyl-3-methylimidazolium based ionic liquids as corrosion inhibitors for mild steel in HCl. *Materials*, 8(6), 3607-3632.
- Mohammed, H. K., Jafar, S. A., Humadi, J. I., Sehgal, S., Saxena, K. K., Abdullah, G. H., ... & Abdullah, W. S. (2023). Investigation of carbon steel corrosion rate in different acidic environments. *Materials Today: Proceedings*
- Ouakki, M., Galai, M., Benzekri, Z., Verma, C., Ech-Chihbi, E., Kaya, S. A. V. A. Ş., ... & Cherkaoui, M. (2021). Insights into corrosion inhibition mechanism of mild steel in 1 M HCl solution by quinoxaline derivatives: electrochemical, SEM/EDAX, UV-visible, FT-IR and theoretical approaches. *Colloids and Surfaces A: Physicochemical and Engineering Aspects*, 611, 125810.
- Ravi, S., Peters, S., Varathan, E., & Ravi, M. (2023). Molecular interaction and corrosion inhibition of benzophenone and its derivative on mild steel in 1 N HCl: Electrochemical, DFT and MD simulation studies. *Colloids and Surfaces A: Physicochemical and Engineering Aspects*, 661, 130919.
- Rbaa, M., Errahmany, N., El Kacimi, Y., Galai, M., El Faydy, M., Lakhrissi, Y., ... & Lakhrissi, B. (2018). Chemical and electrochemical studies of novel quinazolinone derivatives based on 8-hydroxyquinoline as corrosion inhibitor for mild steel in 1.0 M HCl solution. *Anal Bioanal Electrochem*, 10(10), 1328-1354.
- Saha, S. K., & Banerjee, P. (2018). Introduction of newly synthesized Schiff base molecules as efficient corrosion inhibitors for mild steel in 1 M HCl medium: an experimental, density functional theory and molecular dynamics simulation study. *Materials Chemistry Frontiers*, 2(9), 1674-1691.
- Salazar-Jiménez, J. A. (2015). Introduction to Corrosion Phenomena: Types, Influencing Factors and Control for Material's Protection. *Revista Tecnología en Marcha*, 28(3), 127-136.
- Sayyid, F. F., Mustafa, A. M., Hanoon, M. M., Shaker, L. M., & Alamiery, A. A. (2022). Corrosion protection effectiveness and adsorption performance of Schiff base-quinazoline on mild steel in HCl environment. *Corrosion Science and Technology*, 21(2), 77-88.
- Scully, J. R., Glover, C. F., & Santucci, R. J. (2022). | *Electrochemical Tests*.
- Shreir, L. L. (Ed.). (2013). *Corrosion: corrosion control*. Newnes
- Subasree, N., Arockia Selvi, J., & Pillai, R. S. (2023). Effect of alkyl chain length on the corrosion inhibition of mild steel in a simulated hydrochloric acid medium by a phosphonium-based inhibitor. *Journal of Adhesion Science and Technology*, 37(1), 83-104.

- Subasree, N., Selvi, J. A., Arthanareeswari, M., & Pillai, R. S. (2020). Evaluation of tetra-n-butylammonium bromide as corrosion inhibitor for mild steel in 1N HCl medium: experimental and theoretical investigations. *RJC*, 13(01), 499-513.
- Usman, A. D., & Okoro, L. N. (2015). Mild steel corrosion in different oil types. *International journal of scientific research and innovative technology*, 2(2), 9-13.
- Wasim, M., Shoaib, S., Mubarak, N. M., Inamuddin, & Asiri, A. M. (2018). Factors influencing corrosion of metal pipes in soils. *Environmental Chemistry Letters*, 16, 861-879.
- Xu, Z., Cao, X., Wang, Y., Slaný, M., Unčák, S., Li, S., & Tang, Y. (2023). Effective corrosion inhibitor of mild steel in marine environments: Synthesis and application of hydrazides. *Sustainable Materials and Technologies*, 38, e00747.
- Zhao, T., & Jiang, L. (2018). Contact angle measurement of natural materials. *Colloids and Surfaces B: Biointerfaces*, 161, 324-330.